Catalysis Today 181 (2012) 177–183

Contents lists available at ScienceDirect

Catalysis Today

journal homepage: www.elsevier.com/locate/cattod

Carbon formation in catalytic partial oxidation of methane on platinum: Model studies on a polycrystalline Pt foil

Oliver Korup, Robert Schlögl, Raimund Horn*

Fritz Haber Institute of the Max Planck Society, Department of Inorganic Chemistry, Faradayweg 4-6, 14195 Berlin, Germany

ARTICLE INFO

Article history:
Received 27 February 2011
Accepted 29 April 2011
Available online 31 May 2011

Keywords:
Catalytic partial oxidation
Methane
Synthesis gas
Platinum
Carbon
Raman spectroscopy

ABSTRACT

A polycrystalline Pt foil has been investigated as model catalyst in methane catalytic partial oxidation to synthesis gas. It is demonstrated that a substantial amount of carbonaceous deposits forms on the Pt foil upon reaction light-off blocking a large fraction of Pt surface atoms. By using in situ Raman spectroscopy and quantitative spectral analysis the evolution and spatial distribution of these carbonaceous compounds with reaction temperature and reaction time have been characterized. The chemical composition of the carbon material changes from highly reactive and strongly disordered directly after reaction light-off to highly ordered, oxidation and steam reforming resistant after several hours time on stream at 800 °C reaction temperature. Remarkably the carbon distribution at the Pt surface was found to be inhomogeneous and related to the nature of the microcrystals forming the polycrystalline foil in a yet unknown manner.

1. Introduction

The catalytic partial oxidation (CPO) of methane (Eq. (1)) is a potential technology for decentralized conversion of natural gas, consisting mainly of methane, into synthesis gas or hydrogen. In comparison to industrial synthesis gas production by highly endothermic steam reforming (Eq. (2)) carried out in large and cost-intensive tube furnaces, methane CPO is exothermic and can produce synthesis gas yields close to thermodynamic equilibrium in millisecond contact times if proper catalysts are chosen. Due to the high rate and exothermicity, technical CPO reactors could be much smaller than steam reformers and could operate adiabatically as the reaction is self sustained and high temperatures favor synthesis gas production over total oxidation (Eq. (3)).

$$CH_4 + \frac{1}{2}O_2 \rightarrow CO + 2H_2 \qquad \Delta_r H^{\ominus} = -36\,\text{kJ/mol} \tag{1}$$

$$CH_4 + H_2O \rightarrow CO + 3H_2 \qquad \Delta_r H^{\ominus} = +206\,\text{kJ/mol} \tag{2}$$

$$CH_4 + 2O_2 \rightarrow CO_2 + 2H_2O \qquad \Delta_r H^{\ominus} = -803\,\text{kJ/mol} \tag{3}$$

Hickman and Schmidt [1–4] showed that Pt and Rh supported on highly porous α-alumina foam monoliths (porosity >80%) make excellent CPO catalysts due to their low pressure drop at outstanding transport characteristics.

By means of spatial reactor profiles it was later shown by Horn et al. [5] that on both Rh and Pt coated foam catalysts syngas formation can be formally described by a combined oxidation (Eq. (4)) and steam reforming (Eq. (2)) mechanism.

$$CH_4 + \left(2 - \frac{x}{2} - \frac{y}{2}\right) O_2 \rightarrow xH_2 + yCO + (2-x)H_2O + (1-y)CO_2 \qquad \Delta_r H^{\ominus} = f(x, y) \tag{4}$$

Dry (CO_2) reforming, as sometimes reported in the literature, is not observed [6].

Fig. 1 shows a comparion of spatial profiles measured in Rh and Pt foam catalysts for a stoichiometric CH_4/O_2 ratio according to Eq. (1) reproduced from [5] with permission by Elsevier. These profiles were measured at exactly equal conditions (equal metal loading, equal reactant stoichiometry, equal flow rate, equal support) reflecting the difference in the catalytic performance of Rh and Pt. It can be seen that even though species and temperature develop similarly in both foam catalysts quantitative differences exist leading to an overall lower methane conversion and lower syngas selectivity at the end of the Pt foam catalyst compared to the Rh foam catalyst ($X_{CH_4}^{Rh} = 76\%$, $X_{CH_4}^{Pt} = 62\%$, $S_{H_2}^{Rh} = 96\%$, $S_{H_2}^{Pt} = 65\%$, $S_{CO}^{Rh} = 92\%$, $S_{CO}^{Pt} = 73\%$).

While it was demonstrated experimentally [7] and numerically [8–10] for Rh foam catalysts that methane CPO is film transport limited under basically all investigated conditions, it was found that methane CPO on Pt foam catalysts is largely kinetically controlled [5,7]. Indeed it is clearly seen in Fig. 1 that reactant conversion and

---

* Corresponding author.
E-mail address: horn_r@fhi-berlin.mpg.de (R. Horn).

0920-5861/$ – see front matter © 2011 Elsevier B.V. All rights reserved.
doi:10.1016/j.cattod.2011.04.051

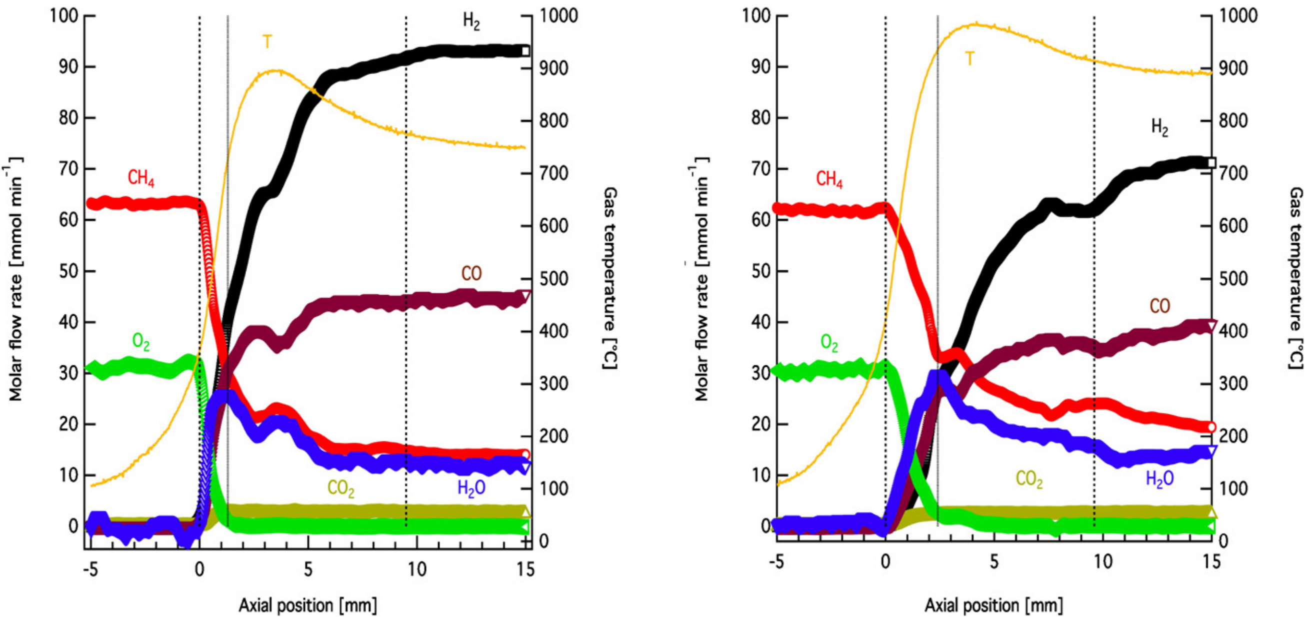

Fig. 1. Comparison of spatially resolved species and gas phase temperature profiles for methane CPO on rhodium and platinum. Left: 5 wt.% Rh supported on an 80 ppi α-alumina foam monolith of about ~10 mm length. Right: 5 wt.% Pt supported on an analog foam monolith. Total inlet gas feed in both cases $\dot{V}_{CH_4} + \dot{V}_{O_2} + \dot{V}_{Ar} = 4700$ mln min^{-1} at 273 K. Inlet stoichiometry C/O = $\dot{V}_{CH_4}/(2\dot{V}_{O_2}) = 1.0$ and $\dot{V}_{Ar}/\dot{V}_{O_2} = 3.76$. Catalyst foam between first and last dotted line. Length of oxidation zone indicated by second dotted line. Data reproduced from [5] with permission by Elsevier.

product formation is much slower on the Pt foam catalyst than on the Rh foam catalyst and the question arises why this is the case.

Giving an answer to this question is of considerable interest not only from a fundamental but also from a practical point of view because it could be that the superior catalytic performance of the Rh foam catalyst in terms of methane conversion and synthesis gas selectivity is solely due to the higher reaction rate leading to pronounced film transport limitation and a very low O_2 concentration at the Rh surface as it was numerically predicted by Dalle Nogare et al. [8]. In this case all surface reactions would proceed at the highest physically possible rate, viz. the rate of species transport to the Rh surface, leading to high methane conversion in the oxidation and steam reforming zone (Fig. 1). In terms of syngas selectivity a low O_2 concentration at the Rh surface leads to high selectivity to partial oxidation products already at the end of the oxidation zone which is then further improved by rapid steam reforming in the steam reforming zone.

This more physical explanation shines a new light onto the selectivity discussion given in the landmark paper by Hickman and Schmidt [1] where the poorer performance of Pt compared to Rh was attributed solely to a difference in the activation barrier for the surface reaction $H^* + O^* \rightarrow OH^*$ of $E_a^{Rh} = 20$ kcal mol^{-1} vs. $E_a^{Rh} = 2.5$ kcal mol^{-1},respectively. It is in fact rather unlikely that such differences in activation barriers have a pronounced influence at temperatures close to 1000 °C and in presence of pronounced film transport limitations such as on Rh.

In the present paper we demonstrate that oxidation and steam reforming resistant carbon deposits form on a Pt surface upon ignition of methane oxidation blocking a large fraction of Pt surface atoms. This observation, even though obtained on a polycrystalline Pt foil as a model system and not yet reproduced for a Pt coated foam catalyst, could be a tentative explanation why methane oxidation and methane steam reforming is significantly slower on Pt compared to Rh with all the catalytic consequences outlined above.

2. Experimental

All experiments were conducted in a temperature controlled in situ reactor cell (Linkam Scientific Instruments, type CCR1000) located under a confocal Raman microscope. The reactor was operated at 1 atm pressure and could be heated up to 1000 °C using a pre-defined temperature program monitored by a thermocouple in direct thermal contact with the reactor sample holder.

A high purity platinum foil was used as model catalyst (Goodfellow Cambridge Limited, 99.99+% purity, polycrystalline ~4 mm × 4 mm × 0.125 mm) mounted on the inner rim of the reactors virtually unreactive ceramic crucible. The platinum foil was cleaned prior to the experiments by repeated rinsing in diluted nitric acid. After placing the foil in the reactor cell it was further cleaned by oxidation at 800 °C (30 min, 20 vol.% O_2 in Ar, 50 mln min^{-1}) followed by reduction at the same temperature (30 min, 20 vol.% H_2 in Ar, 50 mln min^{-1}) and cooling down to room temperature.

Online gas analytics was accomplished by a calibrated mass spectrometer (Pfeiffer Vacuum) in analog scan mode using the Ar peak at $m/z = 40$ as internal standard.

Raman spectra were recorded by a triple filter Raman spectrometer (TriVista S&I GmbH) with a CCD camera (Princeton Instruments) as detector attached to a confocal microscope (Olympus, 10× long-working distance objective), using an Ar$^+$ laser with $\lambda_0 = 488$ nm excitation wavelength (3 mW on the sample). The spectrometer was operated in triple subtractive mode and each spectrum was integrated for 10 min. A two point wavelength calibration was used (laser wavelength and first-order Stokes phonon band of Si at 520 cm^{-1}).

At the applied laser wavelength of 488 nm an intense continuum background occurs at temperatures above 600 °C due to black body radiation from the sample. To overcome this problem an algorithm developed by Gornushkin et al. [11] was adapted to automatically eliminate the continuum background without significantly compromising the spectral integrity in the region of interest. An exemplary spectrum of untreated raw data (black trace), estimated black body background (red trace) and corrected spectrum (blue trace) is depicted in Fig. 2.

For better comparability the baseline corrected spectra were normalized to the G band intensity and fitted depending on the general peak shape. Two cases can be discriminated as shown in Fig. 3. Baseline separated peaks are fitted by two Lorenzian-shaped